Stability of Granular Materials under Vertical Vibrations

Rensheng Deng, Chi-Hwa Wang

Abstract— **The influence of periodic vibrations on the granular flow of materials is of great interests to scientists and engineers due to both theoretical and practical reasons. In this paper, the stability of a vertically vibrated granular layer is examined by linear stability analysis. This includes two major steps, firstly, the base state at various values of mass holdup (M_t) and energy input (Q_t) is calculated and secondly, small perturbations are introduced to verify the stability of the base state by solving the resultant eigenvalue problem derived from the linearized governing equations and corresponding boundary conditions. Results from the base state solution show that, for a given pair of M_t and Q_t, solid fraction tends to increase at first along the layer height and then decrease after a certain vertical position while granular temperature decreases rapidly from the bottom plate to the top surface. This may be due to the existence of inelastic collisions between particles that dissipate the energy input from the bottom. It is also found that more energy input results in a lower solid fraction and a higher granular temperature. The stability diagram is constructed by checking the stability property at different points in the M_t-Q_t plane. For a fixed M_t, the base state is stable at low energy inputs, and becomes unstable if Q_t is larger than a critical value Q_{tc1}. A higher value of M_t corresponds to a larger Q_{tc1}. There also exists a critical mass holdup (M_{tc}), for M_t larger than M_{tc}, the patterns corresponding to the instabilities are standing waves (stationary mode); otherwise the flat layer appears (layer mode). Moreover, the stationary mode turns into the layer mode when Q_t is increased beyond a critical value Q_{tc2}. These findings agree with the experimental observations of other researchers (Hsiau and Pan, 1998). The effects of restitution coefficients (e_p, e_w) and material properties (d_p, ρ_p) on the stability diagram are also investigated. Together with M_t and Q_t these variables can be classified into two groups, i.e. the stabilizing factors (M_t, d_p, ρ_p) and the destabilizing factors (Q_t, e_p, e_w). The stability of the system is enhanced with increasing stabilizing factors and decreasing destabilizing factors.**

Index Terms—**Stability, Granular Materials, Vibrations, Grain Kinetic Theory.**

I INTRODUCTION

GRANULAR materials (sands, grains, catalyst particles, chemical products, etc.) under vertical vibrations are of great interest to engineers and scientists due to practical and theoretical reasons. For instance, shakers are widely used for the mixing, separation and drying processes of particles in industries such as mining, agriculture, construction and chemical engineering. On the other hand, the occurrence of traveling waves (Pak & Behringer, 1993) and standing waves (Umbanhowar, 1997) on the free surface shows the existence of instabilities in this system.

In this paper, a stability analysis method based on the grain kinetic theory, which has been successfully applied to study the instabilities occurring in the shear flow and gravity channel flow (Wang *et al*., 1997; Wang & Tong, 1998, 2001), is adopted to generate an understanding of the instabilities stated above, especially about the determination of the unstable range of operating conditions. To do this, a base state solution is firstly found by solving the macroscopic balance equations based on the grain kinetic theory and secondly, small perturbations are introduced to examine the stability property of the corresponding base state.

II MODEL DESCRIPTION

Figure 1 shows the case to be studied. A bed (height: H_0, mass hold-up: m_p) of granular materials (particle density: ρ_p, particle diameter: d_p) is placed on the top of a vertically vibrated flat plate. The energy flux supplied from the bottom plate to the granular layer is Q_0, and as a result of the vibration the bed expands from its original height to H. In the base state, the materials are activated to move up and down around their own equilibrium position, while the free surface still keeps flat. The zero point of y is set at the center line of the vibrating bottom plate, and the dimensions of x and z are assumed to be infinite because the shape and size of the container do not influence the stability of the system (Melo *et al*., 1994). The movement is

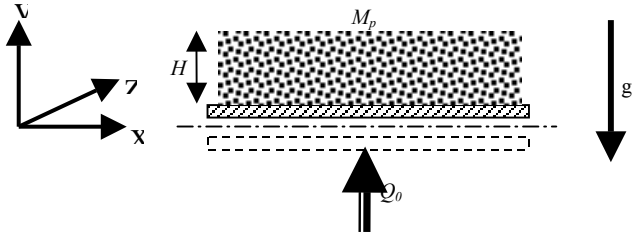

Figure 1 Schematic Diagram of Granular Materials under vertical vibrations.

Rensheng Deng is with Singapore-MIT Alliance, National University of Singapore, 4 Engineering Drive 3, Singapore 117576 (e-mail: smadrs@nus.edu.sg).

Chi-Hwa Wang is with Singapore-MIT Alliance, Department of Chemical and Environmental Engineering, National University of Singapore, 10 Kent Ridge Crescent, Singapore 119260 (e-mail: chewch@nus.edu.sg).

considered as steady, and the mean velocity of particles in each direction is zero. Furthermore, the friction between particles is neglected and only inelastic collisions are left as the particle-particle and particle-wall contact.

The governing equations of mass, momentum and pseudo-thermal energy are those used by Wang *et al*. (1997) and Wang & Tong (1998, 2001)

Continuity: $$\frac{\partial \rho}{\partial t} + \nabla \cdot (\rho \boldsymbol{u}) = 0 \quad (1)$$

Momentum: $$\rho \frac{D\boldsymbol{u}}{Dt} = -\rho \boldsymbol{g} - \nabla \cdot \boldsymbol{\sigma} \quad (2)$$

Energy: $$\frac{3}{2} \rho \frac{DT}{Dt} = -\nabla \cdot \boldsymbol{q} - \boldsymbol{\sigma} : \nabla \boldsymbol{u} - J \quad (3)$$

Here $\boldsymbol{g}$ is the gravity force vector, ρ is the bulk density of the material, given by $\rho = \rho_p \nu$, where ν is the volume fraction of solids. $\boldsymbol{u}$ is the local mean velocity, σ is the stress tensor for the granular assembly and T is the granular temperature, defined as $1/3 \langle \boldsymbol{u}'^2 \rangle$, where $\boldsymbol{u}'$ is the magnitude of the fluctuation about the local mean velocity. $\boldsymbol{q}$ is the flux vector of the pseudo-thermal energy associated with the fluctuations in particle velocity, and J denotes the rate of dissipation of this energy, per unit volume, by inelastic collisions between particles. D/Dt represents the material time derivative following the mean motion. The constitutive relationship for σ, $\boldsymbol{q}$ and J are those of Lun *et al*. (1984).

Boundary conditions at the bottom plate, which take account of momentum and energy transfer between the wall and the materials, are the same as those used by Johnson & Jackson (1987)

$$\boldsymbol{t} \cdot \boldsymbol{\sigma} \cdot \boldsymbol{n} + \left(\frac{\pi \sqrt{3}}{6 \nu_m} \right) \phi' \rho_P \nu g_0(\nu) T^{1/2} u_{sl} = 0 \quad (4)$$

$$\boldsymbol{n} \cdot \boldsymbol{q} = \left(\frac{\pi \sqrt{3}}{6 \nu_m} \right) \phi' \rho_P \nu g_0(\nu) T^{1/2} u_{sl}^2 + Q_0 - \left(\frac{\pi \sqrt{3}}{4 \nu_m} \right) (1 - e_w^2) \rho_P \nu g_0(\nu) T^{3/2} \quad (5)$$

In equations (4) and (5), $\boldsymbol{n}$ is the unit normal to the wall, pointing into the granular material, u_{sl} is the velocity of the granular material in contact with the wall, and $\boldsymbol{t}$ is a unit vector tangent to the wall, in the direction of the slip velocity. The nature of the plate is characterized by ϕ', a specularity factor (which measures the fraction of the momentum of an incident particle in the direction of slip which is transmitted, on average, to the wall in a collision), and e_w, the coefficient of restitution for collisions between particles and the wall. Since the value of u_{sl} is zero for the base state, equation (4) is satisfied trivially.

One boundary condition at the free surface can be obtained by examining the force balance for particles at the top layer, that is, the gravity should be balanced by the supporting force from the materials

$$M \boldsymbol{g} = \boldsymbol{n} \cdot \boldsymbol{\sigma} \cdot a_c \quad (6)$$

Another boundary condition is obtained from the fact that there is no energy input at the free surface, thus

$$\boldsymbol{n} \cdot \boldsymbol{q} = 0 \quad (7)$$

For convenience, the following dimensionless groups are introduced

$$(X, Y, Z) = \frac{(x, y, z)}{H}, \ (U^*, V^*, W^*) = \frac{(U, V, W)}{\sqrt{gH}}, \ T^* = \frac{T}{g d_p}, \ \tau = \frac{t}{\sqrt{H/g}} \quad (8)$$

and

$$M_t = \frac{m_P}{\rho_P d_P}, \ Q_t = \frac{Q_0}{\rho_P (d_P g)^{3/2}} \quad (9)$$

A finite difference method is used here to solve the equations for base state above. The interval of [0,1] in Y-axis is divided into N sub-intervals, and both the equations and boundary conditions are discretized at the grid points. Given the values of M_t and Q_t, the bed height H as well as $\nu(Y)$ and $T(Y)$ for the base state are calculated through an iteration process.

Then, the stability of these steady solutions to small perturbations is studied. Here the motion of the material under vibration is no longer considered to be steady, and the variables of U, V, ν, T in the governing equations (1) - (3) and boundary conditions (4) - (7) are expressed as the base state solutions U_0, V_0, ν_0, T_0 (Note that U_0 and V_0 are zero) plus small perturbations U', V', ν', T'

$$\begin{aligned} U &= U_0(Y) + U' \quad \text{where} \quad U' = U_e(Y) \exp(\Omega \tau) \exp(iK_x X) \\ V &= V_0(Y) + V' \quad \text{where} \quad V' = V_e(Y) \exp(\Omega \tau) \exp(iK_x X) \\ \nu &= \nu_0(Y) + \nu' \quad \text{where} \quad \nu' = \nu_e(Y) \exp(\Omega \tau) \exp(iK_x X) \\ T &= T_0(Y) + T' \quad \text{where} \quad T' = T_e(Y) \exp(\Omega \tau) \exp(iK_x X) \end{aligned} \quad (10)$$

By adopting the same method used by Wang *et al*. (1997), a set of ordinary differential equations in the variables U_e, V_e, ν_e and T_e, subject to two-point boundary conditions, is obtained and constitutes an eigenvalue problem for Ω. This is converted to a matrix eigenvalue problem by taking finite differences, and the resulting eigenvalues are computed with Matlab for a sequence of values of K_x to generate a dispersion relation for each set of values of the physical parameters of the problem. These eigenvalues are then used to determine the stability property of the original base state.

III BASE STATE SOLUTION

The distribution of solid fraction along the Y direction is shown in Fig.2 (a). For a given pair of M_t and Q_t, solid fraction tends to increase at first along the layer height and then decrease after a certain vertical position, forming a peak of density usually at Y_c=0.7~0.9. The occurrence of the densest part in the mid-bed may be due to the joint effects of the energy input from the bottom that scatters the particles and the unbounded movement of particles at the free surface. The

temperature profile along the Y direction is shown in Fig.2 (b). It can be seen that particle temperature decreases rapidly from the bottom to the top as a result of the inelastic collisions between particles that dissipates the energy input from the bottom.

Richman and Martin (1992) calculated the profiles of solid fraction and particle temperature in a vibrating granular materials bed based on the grain kinetic theory. Their results are also compared with this work in Fig.2. Since no direct relationship exists between the energy input Q_t (our parameter) and the dimensionless root mean square velocity V_b (Richman's parameter), the mass holdup (M_t) and the solid fraction at the bottom plate (ν_0) are set identical in order to carry out the comparison. The distribution of granular temperature agrees well, however some differences are observed in the solid fraction profile especially at the free surface. When (M_t, Q_t) = (5.0, 27.7), both models predict a "step change" in solid fraction at the free surface, which remains in our model at (3.0, 19.8) while in Richman's model it turns into a smooth approach to zero. The deviation may be due to the different boundary conditions adopted in these two models: Richman and Martin assumed that the normal stress at the top surface is zero instead of the force balance examination in this work.

However, we do not want to make a judgment about the suitability of the two models. Actually, the base state solution does not always exist in real experiments. If the base state is stable, it can be observed; otherwise, the perturbations existing in the experimental conditions will change the original unstable base state into a new stable one. For example, according to the stability diagram in M_t-Q_t plane (Fig.3), the base state at point (5.0, 27.7) is stable but that at point (3.0, 19.8) is unstable and will evolve into a new state in which the solid fraction smoothly approaches to zero at the free surface as Richman's model suggests (The details will be discussed elsewhere). In this sense, Richman's model may present the final solution, while the base state obtained from this work is an intermediate whose fate depends on the stability analysis.

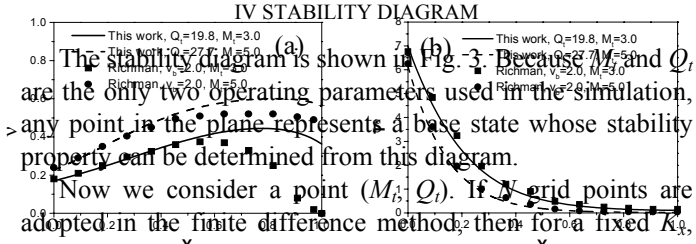

Figure 2 Distribution of (a) solid fraction (b) granular temperature along the bed height at base state.

The stability diagram is shown in Fig. 3. Because M_t and Q_t are the only two operating parameters used in the simulation, any point in the plane represents a base state whose stability property can be determined from this diagram.

Now we consider a point (M_t, Q_t). If N grid points are adopted in the finite difference method, then for a fixed K_x, (4N-7) eigenvalues will be found among which we choose the one with the largest real part of eigenvalue as the *leading eigenvalue*. A group of leading eigenvalues can be obtained by scanning K_x in a wide range, for example, the Ω_r-K_x curve in Fig.4 represents the real part of a set of leading eigenvalues (Ω_r) at different values of K_x. For such a curve, there may be some local maximums, such as the points marked by the circle and the square. The eigenvalues related to these local maximums are called *chief eigenvalues*, among which the one with the largest real part is referred to as the *dominant eigenvalue* (denoted by circle in Fig.4 (a) and square in Fig.4 (b)). If Ω_r corresponding to the dominant eigenvalue is positive, the perturbations in the form of equation (10) will increase exponentially with time in the linear stability analysis, to which we call the base state is "unstable"; otherwise, the perturbations will vanish in the end and keep the present base state unchanged, to which we call the base state is "stable". Here, Ω_r serves as an index for the growth rate of perturbations, and $|\Omega_i|/K_x$ refers to phase velocity.

The solid curves shown in Fig.3 are contours of the real part of chief eigenvalues, with the relevant Ω_r marked nearby. There are obviously two sets of contours: one is named as L set (shown in heavy curves), corresponding to the point marked by circle in Fig.4 where K_x is zero; the other is named as S set (shown in light curves), corresponding to the point marked by square where K_x is positive. These two sets mix together, and contours from one set cross those from the other set. Moreover, all the contours show that the growth rate increases with increasing energy and decreasing mass holdup. Thus, the contours with a Ω_r value of zero form the division between the stable and the unstable area: to the bottom-right of the division are the stable base states, and to the top-left are the unstable base states.

The light dash curve in the diagram consists of the intersections of two contours that have the same value of Ω_r but come from two different sets. That means, any point on this curve has two equal chief eigenvalues, one is in L set and the other is in S set. For any point to the left of the curve, the contour from L set has a larger Ω_r than that from S set, which indicates the Chief eigenvalue from L set (denoted by L-C eigenvalue) is the dominant eigenvalue; for points to the right of the curve, the Chief eigenvalue from S set (S-C eigenvalue) is the dominant eigenvalue.

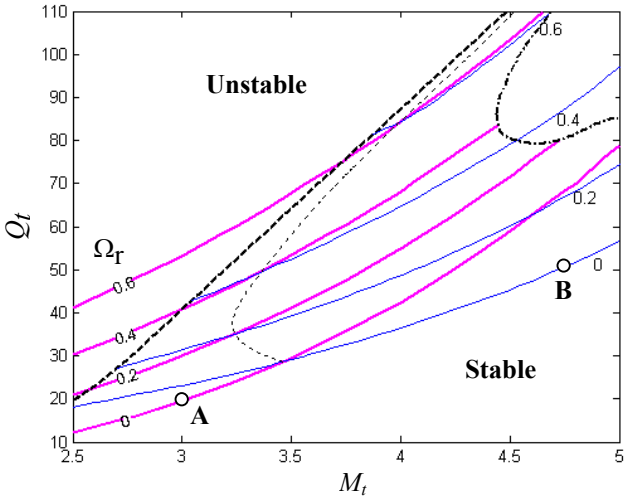

Figure 3 Stability diagram showing the contours of Ω_r. Ω_r =0 refers to the neutral stability contour, Ω_r >0 and Ω_r <0 refer to the unstable and stable regimes, respectively.

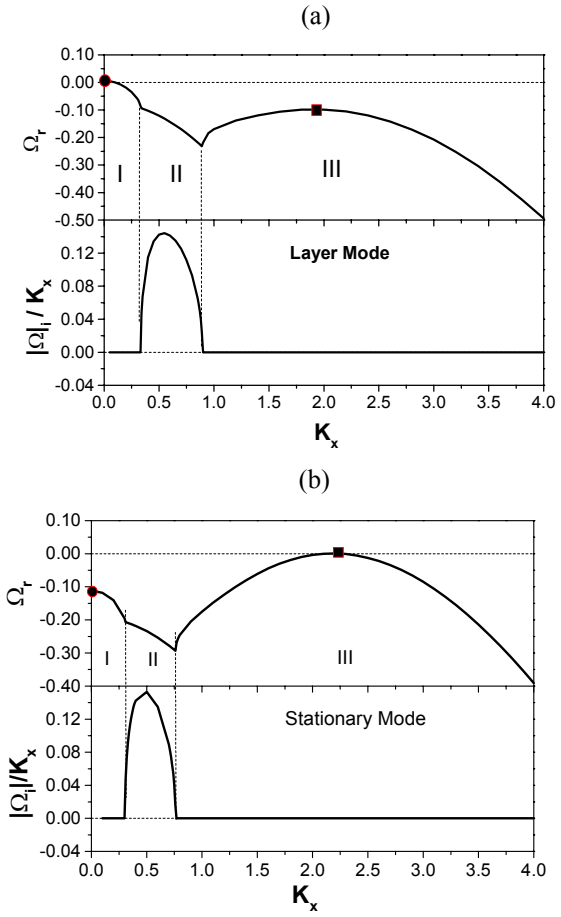

Figure 4 Dispersion relations (a) at point A and (b) at point B, where A and B are indicated in Fig.3.

As stated above, the L-C eigenvalue always appears at the point where K_x is zero. Referring to the perturbation form we adopt in equation (10), it states that the forming new pattern will be unifrom in X direction and only vary along Y dimension. This feature indicates a layer mode. As shown in Fig. 3, the phase velocity related to the S-C eigenvalue is zero, which means the waves are standing and consists the stationary mode. Therefore, the light dash curve is also the division between these two modes: to the left the dominant mode is the layer mode, and to the right is the stationary mode.

However, none of the L set and the S set distributes throughout the whole region. A heavy dash curve in the diagram serves as the beginning of the S set — contours in the S set never appear in the area to the top-left of the heavy dash curve. On the other hand, a heavy dash-dot curve in the top-right of diagram encloses a zone where only the S set exists.

For the mass holdup higher than a critical value M_{tc} (i.e., M_t=4.75), the stationary mode begins to dominate in the M_t-Q_t plane at small energy inputs. Standing waves appear when Q_t is increased over Q_{tc1} = 51.31 while disappear again over Q_{tc2} = 126.45. This agrees well with the experimental observations of Metcalf *et al*. (1997) that for a given frequency, there was an onset acceleration, Γ_{on}, above which ordered wave patterns formed and a higher acceleration, Γ_{off}, beyond which waves were no longer observed. The transition of Q_{tc2} may correspond to the arching state reported by Hsiau & Pan (1998). For a shallow bed with the mass holdup lower than M_{tc}, our model suggests that the flat layer is the dominant pattern without the occurrence of standing waves. This is verified by the experimental results of Melo *et al*. (1994) which stated that the waves disappear when the layer is thin (for their system, the critical dimensionless bed height is H_0/d_p=3).

The effects of e_w and e_p on the stability diagram are also examined. The results show that the energy needed to attain the least-stable state increases with deceasing e_w, as well as the range of stationary mode is enlarged. If the case requiring a higher energy at the least-stable state is regarded as "more stable", the above facts mean that a high value of e_w will destabilize the system. It is also found that e_p has the same effect in destabilization as e_w does. Therefore, it can be concluded that the increase in Q_t, e_p or e_w will cause the base state to be unstable and these variables are referred to as "destabilizing" factors. On the other hand, any change to increase M_t, d_p or ρ_p can suppress the occurrence of instability, thus these parameters are viewed as the "stabilizing" factor here. There is a trade off between these two kinds of opposing factors to decide on whether a base state is stable or not.

V CONCLUSIONS

According to the instability analysis above, base states in the M_t-Q_t plane are classified as stable and unstable regimes, depending on the parameter values (M_t-Q_t). For the stable area, the small perturbations introduced diminish gradually while the unstable area evolves into a new stable base state. The results show that the base state becomes more stable with the increasing stabilizing factor and deceasing destabilizing factor.

ACKNOWLEDGEMENT

This project is supported by National University of Singapore under the grant R-179-000-095-112 and Singapore-MIT Alliance under the grant C382-429-003-091. The authors thank Professor Kenneth A. Smith (MIT) for his valuable advice on the patterns exploration. We also thank Dr. Jingsong Hua for his valuable suggestion on the base state study and Dr. Madhusudana Rao Suryadevara for his help in the preparation of this manuscript. Part of this work has been presented in AIChE Annual Meeting, Indianapolis, Indiana, USA, November 3-8, 2002.

REFERENCES

Hsiau S. S., Pan S. J. *Powder Technol.*, 96, 219-226 (1998)

Johnson, P. C and Jackson, R. 1987. *J. Fluid Mech*. 176, 67-93 (1987)

Lun, C.K.K, Savage, S. B., Jeffrey, D. J., Chepurniy, N. *J. Fluid Mech*., 140, 223-256 (1984)

Melo F., Umbanhowar P. B., Harry L. S. *Phys. Rev. Lett.*, 72(1), 172-176 (1994)

Metcalf T. H., Knight J. B., Jaeger H. M. *Physica A*, 236, 202-210 (1997)

Pak H.K, Behringer R.P. *Phys. Rev. Lett.*, 71, 1832-1835 (1993)

Richman M. W., Martin R. E. *Proceedings of the 9th conference on Engineering Mechanics* (Eds. Lutes, L.D.; Niezzweck, J. N.), 901-903 (1992)

Umbanhowar P. B., *Nature*, 389, 541-542 (1997)

Wang C. H., Sundaresan S., Jackson R. *J. Fluid Mech*., 342, 179-197 (1997)

Wang C. H., Tong Z. *Chem. Eng. Sci.,* 53(22), 3803-3819 (1998)

Wang C. H., Tong Z. *J. Fluid Mech.,* 435, 217-246 (2001)